Methanol-to-Hydrocarbons Product Distribution over SAPO-34 and ZSM-5 Catalysts: The applicability of Thermodynamic Equilibrium and Anderson-Schulz-Flory Distribution

Sahebdelfar, Saeed*+; Yaripour, Fereydoon

Catalysis Research Group, Petrochemical Research & Technology Company, National Petrochemical Company, P.O. Box: 14358-84711 Tehran, I.R. IRAN

Ahmadpour, Somayeh; Khorasheh, Farhad

Department of Chemical and Petroleum Engineering, Sharif University of Technology, P.O. Box: 11365-8639 Tehran, I.R. IRAN

ABSTRACT: *The product distribution of methanol to hydrocarbons conversion over SAPO-34 and ZSM-5 catalysts was studied using thermodynamic equilibrium and Anderson-Schulz-Flory (ASF) distributions. The equilibrium compositions were calculated using constrained Gibbs free energy minimization. The effect of catalyst type was considered by setting upper limits to product carbon number due to shape selectivity according to zeotype catalyst channel size; that is, n≤5 for SAPO-34 but n≤6 for aliphatic and n≤10 for aromatic compounds over H-ZSM-5 catalyst. The equilibrium selectivity of kinds of paraffin is negligible over SAPO-34 system while that of olefins is very small over H-ZSM-5, both in agreement with experimental results for methanol to olefins and to gasoline, respectively. The methanol to olefins hydrocarbon product distributions over SAPO-34 and H-ZSM-5 showed fair agreements with thermodynamic equilibrium and ASF distributions, respectively. It was found that propylene is the only product the selectivity of which can be maximized among hydrocarbon products over both SAPO-34 and ZSM-5 catalysts, and therefore, it can be an easier target molecule in methanol to hydrocarbon conversions.*

KEYWORDS: *Methanol to hydrocarbons, SAPO-34, ZSM-5, Shape selectivity, Equilibrium composition, Anderson-Schulz-Flory distribution.*

INTRODUCTION

The Methanol to Olefins (MTO) reaction has received much attention as a route in natural gas conversions to supply non-petroleum based olefins [1,2]. A simplified stoichiometry is of the form:

$$n CH_3OH \rightarrow (-CH_2-)_n + n H_2O \qquad n \geq 2 \qquad (1)$$

The reaction is exothermic and the degree of exothermicity depends on product distribution. The olefinic

** To whom correspondence should be addressed.*
+ E-mail: s.sahebdel@npc-rt.ir ; sahebdelfar@yahoo.com
1021-9986/2019/2/49-59 11/$/6.01

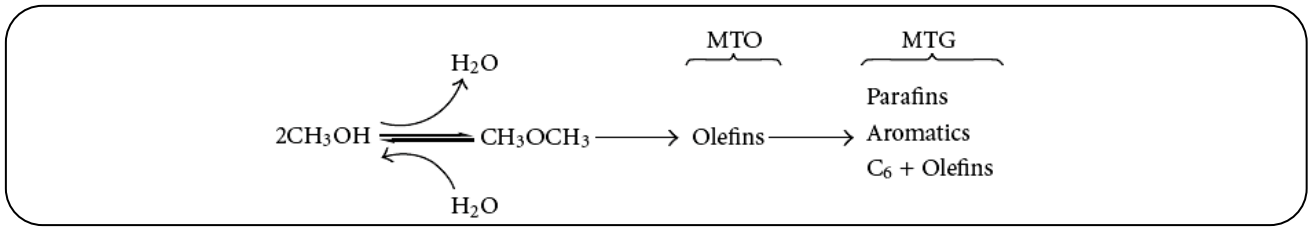

Scheme 1. The reaction path in the conversion of methanol to hydrocarbons over zeolites.

primary products can undergo various side reactions including cracking and hydrogen transfer which reduces olefin selectivity and catalyst life by coke formation. Therefore, the products may be alkenes, cycloalkanes or mixture of alkanes and aromatics [3].

There are many molecular sieve catalysts such as H-ZSM-5, modified Y, mordenite, chabazite, and others that could be used in the conversion of methanol to olefins. The narrow pore SAPO-34 catalyst shows the best performance in terms of activity and selectivity of light olefins, which could achieve 100% methanol conversion and 90% selectivity to light olefins while no C_{6+} hydrocarbons are generated [4].

SAPO-34 is a silicoaluminophosphate molecular sieve with chabazite (CHA) structure, moderate acid strength, 8-membered ring pore entrance, and small pore size (0.43 nm) [5]. The absence of aromatic products appears to be related to the large cavities connected by narrow channels [6]. The pore size is too small to allow the exit of aromatic products, consequently resulting in the accumulation of a large number of organic species in the cavities. Therefore, the catalytic stability is very low due to rapid deactivation by coke formation.

H-ZSM-5 shows much higher stability, although the selectivity of light olefins is much lower. MFI type zeolites are medium pore zeolites with pore size ranging from 0.5–0.6 nm and 10-memebered oxygen ring [7]. The main hydrocarbons formed are C_3–C_5 alkanes and C_6–C_{10} aromatics (mostly methyl substituted benzenes) [3]. The sharp cutoff in product molecular weight over both catalysts is attributed to shape selectivity being governed by the cavity and pore size of the catalyst [8].

During Methanol to Hydrocarbon (MTH) transformation, methanol is firstly dehydrated to dimethyl ether (DME) and subsequently to a variety of hydrocarbons as shown in Scheme 1. Below 300 °C, methanol is mainly dehydrated to DME. The actual reaction network presents a more complicated reaction system in which some reactants and products are reciprocal or overlapped in a series of reactions following different reaction routes [9]. However, for the present work, the simplified reaction scheme (1) suffices.

Many important reactions in C_1 chemistry involving the formation of C-C carbon bonds follow the classic Flory statistics originally developed for free-radical polymerization, but also applicable to step polymerization [10]. Well-known examples include Fischer-Tropsch Synthesis (FTS) [11], synthesis of higher alcohols over Co or Fe based catalysts (often considered as part of FTS) [12], and methane homologation (also known as low-temperature coupling of methane) [3]. It is noticed even in the growth of ultralong carbon nanotubes [13]. Despite their different mechanism and kinetics, these reactions share the step-wise addition of carbon in the forms:

$$C_1 + C_n \rightarrow C_{n+1} \quad (2)$$

$$C_n + C_m \rightarrow C_{n+m} \quad (3)$$

The main reaction path in Methanol to Hydrocarbons (MTH) superficially resembles condensation polymerization of the methanol "monomer" (Eq. (1)), consequently the same statistics for product distribution could be applicable to this reaction. *Wu* and *Kaeding* [14] correlated the product distribution of MTH reaction on ZSM-5 with the conversion of the alcohol. Ethylene was the major primary hydrocarbon produced at low conversions. At higher conversions, the olefins undergo scrambling or thermodynamic equilibration reactions also producing olefin mixtures with good correlation for the Flory equation. Product distributions in the presented experiments showed a significant departure from linearity for the methane and ethylene points, indicating that the formation mechanism of these two compounds are different from those for C_{3+} hydrocarbons.

Tau et al. [15] noted considerable deviations for both C_3 and C_{8+} products. The positive deviation of the latter

was attributed to that once an aromatic ring is formed, aromatic alkylation causes a higher weight fraction of C_8 to C_{10} products to be formed than is anticipated from the ASF plot. Furthermore, it appears that these aromatics are "pseudo-deadend", therefore, they accumulate to a greater extent than anticipated from the ASF plot. The observed deviation might be due to the relatively high contact time they employed.

Cai et al. [16] illustrated the nature of the hydrocarbon pool (HCP) from a thermodynamic aspect and proposed an equilibrium analysis of methylbenzene intermediates for a methanol-to-olefins process which followed a pseudo Anderson–Schulz–Flory (ASF) olefin distribution under commercial operating conditions. The experimental product distribution results over ZSM-5 zeolites were found to follow the ASF distribution, with ethylene as an exception. They concluded that this type of distribution can only exist under quite high conversion conditions and the space velocity has to be near commercial practice.

Liu et al. [17] studied the thermodynamics of MTH and compared the results with that over nano H-ZSM-5 (Si/Al =25 and 60) catalysts. Simulations were performed without solid carbon (coke), CO, CO_2, and light alkanes, selecting 25 reactions incorporating C_1–C_9 components and their intra-conversions (H transfers). It was noted that when coke, CO, CO_2, and gaseous alkanes were ignored, the simulated results were closer to those have been observed in a real time-on-stream MTH reaction. Furthermore, in the case that intra-conversions were ignored, due to limited product dwelling time, thermodynamic calculation showed fairly close results to the real experimental data. Their work illustrates the importance of proper choosing the products and/or reactions for a rational thermodynamic prediction of MTH product distribution.

Methanol itself is a valuable feedstock; therefore, the economy of the MTH processes strongly depends on product selectivity, with light olefins being the most desirable products. Therefore, the investigation of product distribution could give a good insight into the development of methanol-based processes. To the best of our knowledge, no systematic work on product distribution reflecting the effect of catalyst type and operating conditions have been published.

In this work the product selectivity and distribution in MTH over SAPO-34 and ZSM-5 catalysts were studied using both thermodynamic and kinetic considerations. The equilibrium dehydration of methanol to DME and hydrocarbons was studied using constrained Gibbs free energy minimization method. The applicability of the Anderson-Schulz-Flory distribution on MTO product distribution was investigated. Also, the effect of catalyst type and operating conditions on product distribution was studied.

EXPERIMENTAL SECTION

Experimental

The commercial ZSM-5 catalyst was supplied by a Chinese company. The H-ZSM-5 (catalyst A) and H-[B]-ZSM-5 (catalyst B) zeolites were prepared by hydrothermal synthesis according to the following procedure. Calculated amounts of sodium aluminate, silicic acid, sodium hydroxide, tetrapropyl ammonium bromide (TPABr), boric acid and deionized water were mixed and stirred to form a gel with molar ratios of $20SiO_2$: $0.05Al_2O_3$: xB_2O_3: 1TPABr:$1.5Na_2O$: $200H_2O$ (x = 0, 1 for samples A and B, respectively). Crystallization was carried out at 180 ºC under autogenous pressure in an autoclave for 48 h. The product was filtered, washed and dried at 105 °C overnight and then calcined under air flow at 530 °C for 12 h. The parent ZSM-5 zeolites were turned into the H-form by ion-exchange with 1 mol/L NH_4NO_3 solution at 80 °C for 5 h, followed by filtration, washing and drying at 105 °C for 12 h and calcination at 530 °C for 12. The resulting powders were formed by tableting and then 16–25 mesh catalysts were made by crushing and sieving for catalytic evaluation in the reactor.

The porous structure of the catalysts was determined by N_2 adsorption–desorption (Quantachrome NOVA 2200). The acidity of the catalysts was determined by adsorption-desorption of NH_3, using a BELCAT-A instrument. Table 1 summarizes the characterization results of the catalysts. It shows that the commercial sample was a mesoporous (or hierarchical) zeolite.

Methanol to olefins reactions over the ZSM-5 samples were carried out in a fixed-bed reactor (450 mm length, 11 mm I.D). In a typical run, 4 g of each catalyst was loaded into the reactor and methanol–water mixture (mass ratio 1:1) was fed to provide a methanol weight hourly space velocity (WHSV) of 0.9 h^{-1}. The reaction temperature and pressure were 480 ºC and 1 bar, respectively.

Table 1: Physical properties and acidity of the catalysts.

Sample Name	Physical properties					Acidity (mmole of $NH_3/g_{Cat.}$)		
	Si/Al ratio[a]	S_{BET} $(m^2/g)^b$	V_{Total} $(cm^3/g)^c$	V_{Micro} $(cm^3/g)^d$	V_{Meso} $(cm^3/g)^e$	Weak	Strong	Total
Commercial MTP catalyst	175	355	0.279	0.108	0.171	0.205	0.175	0.380
Catalyst A (No boron)	190	408	0.213	0.164	0.049	0.093	0.122	0.215
Catalyst B (With boron)	190	404	0.214	0.157	0.057	0.144	0.109	0.253

a) Determined by inductively coupled plasma (ICP) spectroscopy, b) Total surface areas were obtained by the BET method using adsorption data in P/P_0 ranging from 0.05 to 0.25, c) Total pore volumes were estimated from the adsorbed amount at $P/P_0 = 0.99$, d) Measured by t-plot method using adsorption data in P/P_0 ranging from 0.19 to 0.39, e) $V_{meso} = V_{ads,\ p/po=0.99} - V_{micro}$

The gas-phase products [(CH_4, C_2–C_5 olefins/paraffins, DME, C_6-cut) and (H_2, CO, and CO_2)], aqueous part and organic portion of the liquid product were analyzed by gas chromatographs. More details of preparation, characterization and performance tests can be found elsewhere [18].

The experimental conversion and selectivity data for SAPO-34 catalyst were obtained from the appropriate literature.

Equilibrium calculations

For a given *T*, *P* and initial feed, the equilibrium compositions of a reacting system can be obtained by minimization of its total Gibbs energy, G^t, according to Eq. (4):

$$dG^t_{T,P} = 0 \qquad (4)$$

The objective function is subject to the constraining conservation of the total number of atoms of each element in a system comprised of *w* elements. The material balance for the element *k* is then:

$$\sum_i n_i a_{ik} - A_k = 0 \qquad (k = 1,2,...w) \qquad (5)$$

Where n_i is the moles of chemical species *i*, a_{ik} is the number of atoms of the *k*th element present in each molecule of species *i* and A_k is the total number of atomic masses of the *k*th element in the feed. Taking the partial derivatives of the Lagrange function, *F*;

$$F = G^t + \sum_i \lambda_k \left(n_i a_{ik} - A_k\right) = 0 \qquad (6)$$

In which λ_k is a Lagrange multiplier, with respect to n_i and setting equal to zero, the following equations can be obtained for gaseous systems [19]:

$$\Delta G^0_{fi} + RT \ln \frac{y_i \hat{\phi}_i P}{P^0} + \sum_k \lambda_k a_{ik} = 0 \qquad (i = i,2,...N) \qquad (7)$$

Where P^0 is the standard pressure, and y_i and $\hat{\phi}_i$ are the mole fraction and fugacity coefficient of species *i*, respectively. For low pressures or high temperatures, as is the case for the present work, the ideal gas assumption is adequate. The choice of a set of species is entirely equivalent to the choice of a set of independent reactions among the species.

The limitations imposed by shape selectivity on products were considered as additional constrains in thermodynamic simulation. As a consequence, the components used for equilibrium calculations over SAPO-34 catalyst were methanol, DME, water, and C_1–C_5 paraffins and olefins. For ZSM-5 simulations, 20 compounds were considered in equilibrium calculations, namely, methanol, DME, water, methane, ethane, propane, *i*-butane, *i*-pentane, *i*-hexane, ethylene, propylene, 1-butene, trans-2-butene, trans-2-pentene, trans-2-hexene, benzene, toluene, *p*-xylene, mesitylene (1,3,5-trimethyl benzene) and durane (1,2,4,5-tetramethyl benzene). The isomers were lumped as one of the more stable ones (e.g., iso-alkanes and cis-2-olefins) having more probability of formation as listed above. The required Gibbs free energies of formation were obtained from the literature [20] and the resulting set of non-linear Equations (5) and (6) was solved by Matlab software using a quasi-Newton method.

It is noteworthy that due to the sieving effect of the channels, other (bulkier) products may also be present within zeotype cages. According to the so called hydrocarbon pool mechanism [21], methanol is first dehydrated to 'hydrocarbon-pool'= $(CH_2)_n$ representing adsorbate which can be converted to C_2-C_4 olefins

(in SAPO-34 catalyst) via reversible parallel paths as well as paraffin and coke by-products. As long as the turn-over rate of methanol is much higher than that of net growth of these species (which should be the case for a practical catalyst), these intermediate species could not affect the external equilibrium product composition because of the point function nature of thermodynamic properties. Consequently, it is not necessary to include them in equilibrium calculations.

The Anderson-Schulz-Flory distribution for product selectivity is commonly used in the form:

$$\frac{W_n}{n} = \frac{(1-\alpha)^2}{\alpha}\alpha^n \quad (8)$$

Where W_n is the weight fraction of hydrocarbons containing n carbon atoms and α is the chain growth probability. A semi-log plot of Eq. 8 gives a straight line with a slope of α. The larger the chain growth probability, the heavier are the hydrocarbon products.

RESULTS AND DISCUSSION

Equilibrium calculation results

An advantage of equilibrium analysis is that no detailed reaction mechanism is necessary and reactions pathway, largely governed by catalyst type, suffices. It also provides a limit for conversion and product distribution. The results of thermodynamic calculations are given below.

SAPO-34 catalyst

Fig. 1 shows the equilibrium carbon-based selectivity of different products as a function of temperature at 1 bar over SAPO-34 catalyst. The selectivity of C_2 and C_3 olefins increases with temperature whereas that to C_4 and C_5 olefins decreases with temperature. This shows that higher reaction temperatures favor the formation of lower alkenes thermodynamically, especially ethylene. This can be explained by the endothermic nature of cracking reactions that favor the formation of lower hydrocarbons at higher temperatures.

Fig. 2 illustrates the effect of pressure on the equilibrium selectivity of products at 450 °C. An increase in the pressure lowers the equilibrium selectivity of ethylene and propylene while it increases that of C_4 and C_5 olefins. This can be attributed to the smaller volume expansion factor for higher olefins formation (Eq. (1)).

Fig. 3 displays the effect of water content in the initial feed on product selectivities. Water vapor is commonly used for temperature control and also as an *in situ* coke removing agent [22]. A comparison of Figs. 2 and 3 reveals that although water is involved in equilibria among oxygenates and hydrocarbons, it behaves in similar manner to inert diluents through decreasing the partial pressure of the reacting species. This implies that the dehydration reactions to hydrocarbons are essentially irreversible. Similarly from a kinetic point of view, high Si/Al zeolites are hydrophobic and show little affinity for water molecules especially at higher temperatures. Thus water molecules should exhibit little effect on catalytic site activity.

Under conditions for which Figs. 1–3 are plotted, the equilibrium methanol conversions are nearly complete with very small selectivity of DME indicating the dehydration reactions are highly favored under typical MTO reaction conditions. The carbon containing part of the products comprises only olefins and selectivity of kinds of paraffin (even methane!) is negligibly small.

ZSM-5 catalyst

Fig. 4 shows the equilibrium product selectivity versus temperature at 1 bar for H-ZSM-5 catalyst. The equilibrium products are paraffin and aromatics with little olefins. Unlike SAPO-34, the product composition is slightly affected by temperature. An increase in temperature from 250 to 450 °C results in a decrease of alkylbenzenes/aromatics equilibrium molar ratio from 0.2 to 0.07 which illustrates that higher temperatures favor dealkylation reactions. The equilibrium product composition for methanol to hydrocarbons over H-ZSM-5 zeolites is closer to MTG than to MTO. Therefore, to obtain light olefins over ZSM-5, the reaction should be controlled kinetically (e.g., by using high space velocities).

The paraffinic products consist mainly of methane (99.9 mole % at 450 °C and 1bar), while in the aromatic cut, benzene is the main constituent (92.7 mole %), proposing the following stoichiometric reaction:

$$9CH_3OH \Leftrightarrow 3CH_4 + C_6H_6 + 9H_2O \quad (9)$$

Equation (9) is highly undesirable because it brings about wasting more than 30% of carbon in methanol feed as methane.

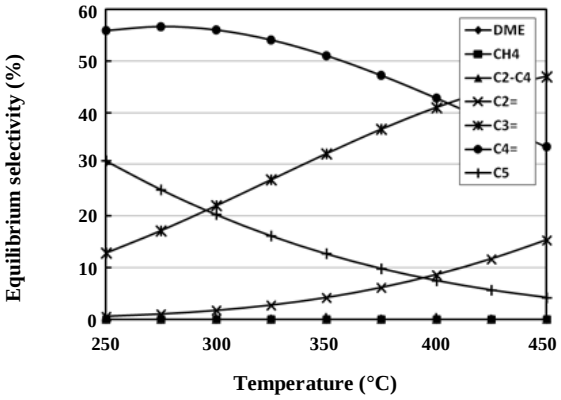

Fig. 1: Equilibrium selectivity of products versus temperature (at 1 bar) for SAPO-34 catalyst (methanol conversion ≈1).

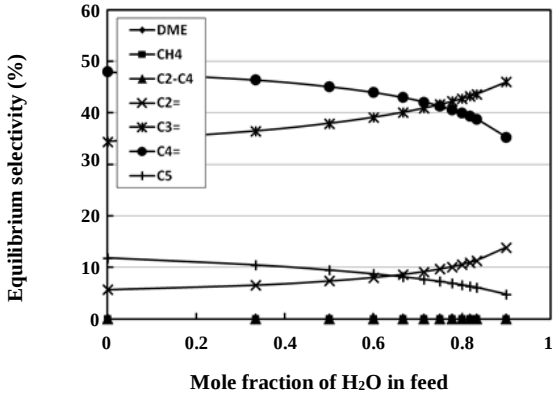

Fig. 3: Equilibrium selectivity of products versus mole fraction of water in initial feed (at 450 °C and 10 bar) for SAPO-34 catalyst (methanol conversion ≈1).

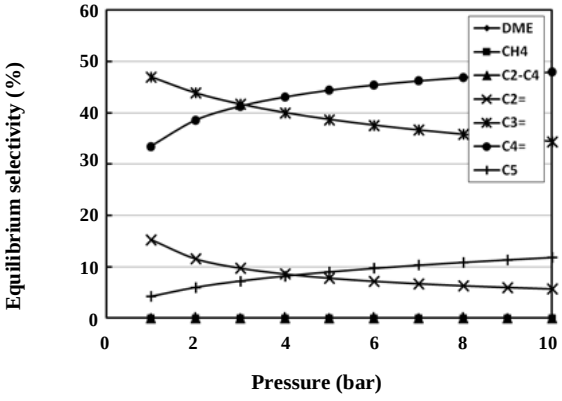

Fig. 2: Equilibrium selectivity of products versus pressure (at 450 °C) for SAPO-34 catalyst (methanol conversion ≈1).

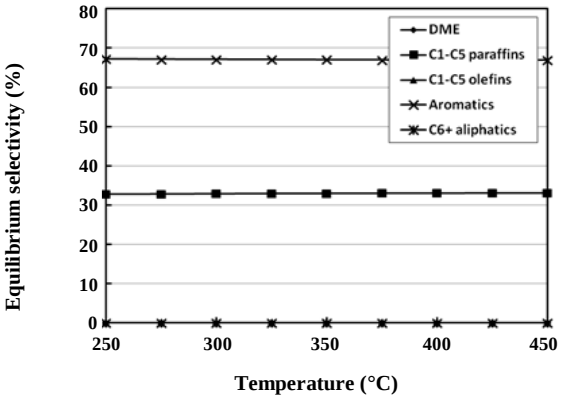

Fig. 4: Equilibrium products selectivity versus temperature for ZSM-5 catalyst at 1 bar (methanol conversion ≈1).

Fig. 5 presents the equilibrium product selectivity versus pressure at 450 °C for ZSM-5 catalyst. The product composition is also slightly affected by the pressure. An increase in pressure from 1 to 10 bar results in an increase of alkylbenzenes/aromatics molar ratio from 0.07 to 0.18. The equilibrium molar ratio of olefins/paraffins, however, decreases with increasing pressure. Both of these trends were observed in practice [23].

Comparison with experimental results

Table 2 compares the equilibrium selectivity results of thermodynamic simulation with typical experiments over SAPO-34 under the same conditions. The equilibrium C_2-C_4 olefin selectivity is very close to the corresponding experimental value; however, individual olefin selectivities show some deviations. Propylene is the thermodynamically favored product. A comparison of equilibrium and experimental selectivities reveals that the equilibrium selectivity of ethylene is lower than the experimental value over SAPO-34 in contrast to butenes selectivity. This is the case for most other experimental works (e.g., [24-26]). This could be due to the fact that in catalyst evaluation tests maximum light olefins are sought for which the reaction condition, e.g. high space velocities, are set accordingly. Lower experimental ethylene selectivities (~20 %) and higher butene selectivities (>20%) at the same temperature have been also reported [6], illustrating that ethylene could be dimerized to butenes shifting the product selectivities to near equilibrium values.

The very low equilibrium selectivity of alkanes and C_5 aliphatic hydrocarbons agrees well with the experimental results. Although the formation of C_1-C_5 paraffins

Table 2: Comparison of equilibrium and experimental MTO results on 3% Y- modified SAPO-34.

Method	Selectivity (%)						
	C_1	C_2-C_4	$C_2^=$	$C_3^=$	$C_4^=$	C_5	$C_2^=$-$C_4^=$
Experimental [23]	0.5	5.1	46.2	37.2	7.8	3.2	91.2
Simulated	≈0	≈0	13.3	45.6	36.0	5.1	94.9

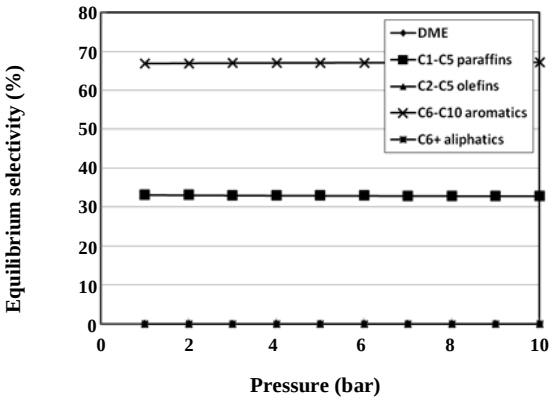

Fig. 5: Equilibrium products selectivity versus pressure for ZSM-5 catalyst at 450 °C (methanol conversion ≈1).

on SAPO-34 is not hindered by shape selectivity, the hindrance of net formation of bulkier aromatic products reduces the hydrogen transfer activity and thereby formation of kinds of paraffin. The results are also consistent with the observed very high selectivity to olefins.

Table 3 compares hydrocarbon selectivities on a lump basis over ZSM-5 zeolite to that reported in the literature for MTG reaction [27]. The experimental results showed that methane and ethane comprise only a small proportion of the products, unlike the equilibrium product composition. Elimination of these two components from simulation (that is, considering a metastable equilibrium condition) significantly improves the simulation results (Table 3).

Non-equilibrium product distribution

The highly undesirable equilibrium product selectivity over medium pore zeolites implies that the reaction should be operated under kinetically controlled regime where the equilibrium selectivity results are not applicable.

Equation (1) and Scheme 1 suggest that an ASF distribution type could be applicable to MTO reaction. Fig. 6 depicts the ASF plot of our experimental results for C_1–C_{10} products of MTO reaction over ZSM-5 catalyst samples under the kinetically controlled regime. Methane and C_2 products showed negative deviations from ASF distribution indicating a different formation mechanism for these two compounds [28], whereas C_3-C_{10} hydrocarbons showed favorable fits. Methane is formed directly from dimethylether or methanol, but also from the demethylation of polymethylbenzenes or of coke molecules [29], although demethylation reactions are not important due to their low equilibrium constants [30]. Ethylene could form via ethanol intermediate [3]. The high selectivity of C_3 (Fig. 6.a) has been the basis for on-purpose propylene production from methanol in Lurgi (now Air liquid) MTP and NPC-RT PVM processes.

The slopes correspond to chain growth probabilities of 0.53, 0.47 and 0.52 for catalysts A, B, and commercial catalysts, respectively. Boron increases the catalyst stability at the expense of its activity by reducing the acidity to moderate acidity [18] which can account for the lower numerical value of α for boron incorporated catalyst B. A comparison of chain growth probabilities for commercial and Sample A catalysts reveals similar α values despite the stronger acidity of the former. This implies that introducing mesoporosity to the zeolite compensated the promoting effect of its higher acidity on the α value through reducing intraparticle methanol-catalyst contact time resulted from facilitated mass transport in the mesopores. This illustrates the beneficial effect of mesoporosity of the zeolite on selectivity to lower alkenes. Similarly, over a given catalyst, factors favoring lower olefins formation such catalyst deactivation, higher temperatures and space velocities, and lower pressures should decrease α.

The effect of shape selectivity on the selectivity and activity of ZSM-5 in MTO reaction on C_{10+} hydrocarbons largely excludes them from product profiles. Consequently, the ASF distribution is expected to be limited to C_3-C_{10} hydrocarbons when lower olefins (C_2–C_4) constitute the main products (i.e., > 80 wt% of MTO products) and shape selectivity is not still a determining factor.

Table 3: Comparison of equilibrium and experimental MTH results on ZSM-5 catalyst.

Method	Selectivity (%)								
	paraffins	olefins	C_{6+} aliphatic	aromatics					
				benzene	toluene	Ethyl-BZ	xylenes	C_{9+} aromatics	Total
Experimental [27]	49.1	3.3	4.3	1.8	11.1	0.8	18.1	11.5	43.3
Simulated	33.0	≈0	≈0	60.4	6.5	0.02	0.05	≈0	67.0
Simulated (ignoring CH_4 and C_2H_6)	57.6	0.25	7×10^{-3}	15.3	23.0	0.82	2.5	0.53	42.2

** T=371 °C, p=1 atm, experimental and equilibrium conversions≈100 (slectivities smaller than 1×10^{-3} are denoted as ≈0).*

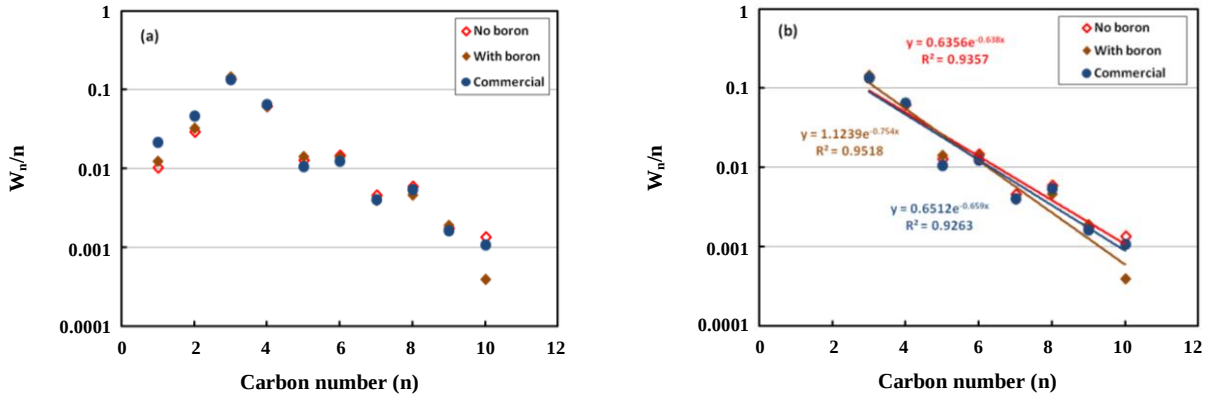

Fig. 6: Anderson-Schulz-Flory plots for samples A and B (average values after 900 h) and commercial (average values after 350 h) H-ZSM-5 catalysts (a) C_1-C_{10} products (b) C_3-C_{10} products (T=480 ºC, p=1 bar, WHSV=0.9 h^{-1}). The order of fitted equations from top to bottom is the same as that of the legends.

Wu and *Kaeding* [14] obtained fair fits for C_3-C_9 products with α=0.5-0.6 for nearly complete methanol conversions over H-ZSM-5 zeolites with various SiO_2/Al_2O_3 ratios (35-1600), although excellent fits were obtained only for lower methanol conversions. The α value in their work is in good agreement with the results of the present work. Furthermore, it appears that for α values below 0.6 (high selectivity to propylene) ASF distribution is applicable to the results. They also observed a significant departure from linearity for the ethylene point in all the runs with ZSM-5 with the highest silica/alumina ratios. The deviation was attributed to the formation of ethylene by a different mechanism than propylene and other hydrocarbons.

Despite the fact that MTO is not a simple polymerization reaction and the complexity of its mechanism, it is remarkable that the ASF product distribution is observed at all. The prevalence of ASF product distribution would favor a consecutive type mechanism with one carbon from methanol adding during each step. An alternative parallel type mechanism, known as the "hydrocarbon-pool" (HCP) mechanism has been suggested by *Dahl* and *Kolboe* [21], who studied the methanol to hydrocarbons conversion using SAPO-34 as a catalyst.

The nature of HCP species has been investigated intensively and studies have proved that methylbenzenes are the HCP species in MTO reaction on SAPO-34 and revealed the correlation between the presence of methylbenzenes in SAPO-34 cages and the formation of olefin products [9].

The ASF distribution, however, would not be applicable to SAPO-34 catalyst because shape selectivity becomes a dominant factor very early during the scrambling of the molecular weight of products and limits the products to C_5 and lower hydrocarbons.

Ultimate product distribution

The findings of this work suggest that the ultimate (equilibrium) methanol dehydration products over

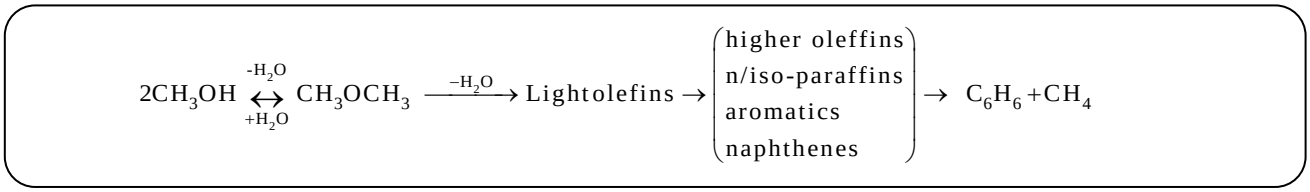

Scheme 2: The reaction path of methanol to hydrocarbons extended to ultimate products.

medium pore zeolites, in addition to water, would be benzene and methane. Consequently, the reaction scheme 1 could be extended as shown in Scheme 2.

Methane could result from both a direct transformation of dimethyl ether and from a secondary reaction. A hydride transfer between methoxy species and dimethyl ether or methanol could explain the direct pathway [31]. At high conversions (long contact times), methane could also result from the protolytic cracking of alkanes [32].

The demethylation of desorbed aromatics is also a possible mode of methane formation. This is supported by the observation that, distribution of aromatics changes from pentamethyl- and hexamethyl-benzenes at low conversion to less alkylated benzenics at high conversion (tetramethylbenzenes, trimethylbenzenes, xylenes, and toluene). However, the increase in the degree of alkylation at high DME conversion could also be caused by a lack of methylating species (dimethyl ether, methanol).

As mentioned above, methyl substituted benzenes are the main aromatic homologs of benzene which can undergo dehydro-demethylation in the presence of water over acidic sites, which eventually shifts the product selectivity to benzene and methane.

Transport limitation effects

The results of this work predict that over SAPO-34 and micropore zeotypes, in which thermodynamic equilibrium plays an important role, the selectivity of olefins should be independent of catalyst size and space velocity as long as oxygenate (methanol and DME) conversions are very high. These have been supported by experimental works.

Chen et al. [33] observed that the selectivity of different olefins was independent of the crystal size at relatively low coke contents (less than 10 wt.%) over SAPO-34 of crystal sizes in the range 0.25–2.5 mm. It should the out that higher coke contents influences shape selectivity and thus product selectivity. Similar results have been obtained by other workers [34,35]. Below 500 nm diameter crystal size diffusion limitations are not significant in SAPO-34 catalysts [36].

Chen et al. [37] found that MTO reactions for SAPO-34 larger than 2.5 μ are diffusion limited which is enhance by catalyst deactivation. Therefore, the reaction rate within the catalyst pores could be much faster than the rate at which species enter and leave the pores. As a consequence, the composition inside the pores can be closer to equilibrium than that of the bulk fluid. This could account for the deviation observed from thermodynamic equilibrium on SAPO-34 catalysts.

Similarly, *Wu et al.* [35] observed that the methanol weight hourly space velocity (MWHSV) higher than 0.54 h^{-1}, the effect of MWHSV on $C_2^=$–$C_4^=$ selectivity is quite insignificant over SAPO-34 catalysts, and the selectivity remains steady with time on stream. However, the catalyst deactivates faster at 0.54 and 6.00 h^{-1} than other space velocities. Therefore, MWHSV of 1.6–3.6 h^{-1} may be an optimal range for the MTO process.

On the other hand, the prevailing ASF distribution in ZSM-5 catalyzed reaction implies that crystallite size and residence should have a significant influence on product distribution. Smaller crystallites and shorter residence time favor formation of lower olefins. The can be achieved by using nanozeolites or hierarchical ZSM-5 catalysts.

CONCLUSIONS

The product composition in methanol to hydrocarbons process is very complex and variable and cannot be explained by any single product distribution model. However, under limiting cases, available models are capable of giving reasonable fits. According to the findings of this work, some main conclusions are as follows:

The equilibrium product selectivity over SAPO-34 favors the formation of propylene above 400 °C.

The equilibrium product selectivity over ZSM-5 is mostly methane and benzene (nearly 3/1 molar ratio).

The predicted equilibrium composition and selectivity over SAPO-34 show better agreement with experimental data as compared with ZSM-5.

Over medium pore zeolites such as ZSM-5, the C_3–C_{10} product distribution of MTO reaction follows Anderson-Schulz-Flory distribution under kinetically controlled conditions.

Promotion of ZSM-5 catalyst with boron to improve its stability decreases the chain growth probability in MTO reaction implying higher selectivity of lower molecular weight olefins.

Both SAPO-34 and ZSM-5 catalysts can be employed for the production of propylene as the main hydrocarbon product, although under different operating conditions.

Acknowledgements

The authors would like to acknowledge the Petrochemical Research and Technology Company of the National Petrochemical Company (Tehran/Iran) for their financial support of this study. Also, financial support by the Research Office of Sharif University of Technology (Tehran/Iran) is gratefully appreciated.

Received : Aug. 17, 2017 ; Accepted : Feb. 26, 2018

REFERENCES

[1] Sousa-Aguiar E.F., Appel L.G., Mota C., Natural Gas Chemical Transformations: The Path to Refining in the Future, *Catal. Today*, **101**: 3-7 (2005).

[2] Wu W., Guo W., Xiao W., Luo M., Dominant Reaction Pathway for Methanol Conversion to Propene over High Silicon H-ZSM-5, *Chem. Eng. Sci.*, **66**: 4722-4732 (2011).

[3] Olah G.A., Molnár Á., "Hydrocarbon Chemistry", 2nd ed., John Wiley & Sons, Inc., New York (2003).

[4] Qi G., Xie Z., Yang W., Zhong S., Liu H., Zhang C., Chen, Q., Behaviors of Coke Deposition on SAPO-34 Catalyst during Methanol Conversion to Light Olefins, *Fuel Process. Technol.*, **88**: 437-441 (2007).

[5] Wang P., Lv A., Hu J., Xu J., Lu G., In Situ Synthesis of SAPO-34 Grown onto Fully Calcined Kaolin Microspheres and Its Catalytic Properties for MTO Reaction, *Ind. Eng. Chem. Res.*, **50**: 9989-9997 (2011).

[6] Yang G., Wei Y., Xu S., Chen J., Li J., Liu Z., Yu J., Xu R., Nanosize-enhanced Lifetime of SAPO-34 Catalysts in Methanol-to-Olefin Reactions, *J. Phys. Chem. C*, **117**: 8214-8222 (2013).

[7] Karge H.G., Hunger M., Beyer H.K., Chapter No. 4: Characterization of Zeolites-Infrared and Nuclear Magnetic Resonance Spectroscopy and X-Ray Diffraction, in: Weitkamp, J., Puppe L., (eds.), "Catalysis and Zeolites: Fundamentals and Applications", Springer -Verlag Berlin (1999).

[8] Olsbye U., Svelle S., Bjørgen M., Beato P., Janssens T.V.W., Joensen F., Bordiga S., Lillerud K.P., Conversion of Methanol to Hydrocarbons: How Zeolite Cavity and Pore Size Controls Product Selectivity, *Angew. Chem. Int. Ed.*, **51**: 5810-5831 (2012).

[9] Tian P., Wei Y., Ye M. Liu, Z., Methanol to Olefins (MTO): From Fundamentals to Commercialization, *ACS Catal.*, **5**: 1922-1938 (2015).

[10] Fogler H.S., "Elements of Chemical Reaction Engineering", 3rd ed., Prentice Hall, New Jersey (1999).

[11] Speight J.G., "Handbook of Industrial Hydrocarbon Processes", Elsevier, Amsterdam (2010).

[12] Kiennemann A., Idriss H., Kieffer R., Chaumette P., Durand D., Study of the Mechanism of Higher Alcohol Synthesis on Copper-zinc Oxide-aluminum Oxide Catalysts by Catalytic Tests, Probe Molecules, and Temperature Programmed Desorption Studies, *Ind. Eng. Chem. Res.*, **30**: 1130-1138 (1991).

[13] Zhang R., Zhang Y., Zhang Q., Xie H., Qian W., Wei F., Growth of Half-meter Long Carbon Nanotubes Based on Schulz-Flory Distribution, *ACS Nano*, **7**: 6156-6161 (2013).

[14] Wu M.M., Kaeding W.W., Conversion of Methanol to Hydrocarbons: II. Reaction Paths for Olefin Formation over HZSM-5 Zeolite Catalyst, *J. Catal.*, **88**: 478-489 (1984).

[15] Tau L-M., Fort A.W., Bao S., Davis B.H., Methanol to Gasoline: ^{14}C Tracer Studies of the Conversion of Methanol/Higher Alcohol Mixtures over ZSM-5, *Fuel Process. Technol.*, **26**: 209-219 (1990).

[16] Cai D., Wang Q., Jia Z., Ma Y., Cui Y., Muhammad U., Wang Y., Qian W., Wei F., Equilibrium Analysis of Methylbenzene Intermediates for a Methanol-to-Olefins Process, *Catal. Sci. Technol.*, **6**: 1297-1301 (2016).

[17] Liu B., Yao B., Gonzalez-Cortes S., Kuznetsov V.L., AlKinany M., Aldrees S.A., Tiancun Xiao, Peter P. Edwards, A Research into the Thermodynamics of Methanol to Hydrocarbon (MTH): Conflictions between Simulated Product Distribution and Experimental Results, *Appl Petrochem Res.*, **7**: 55–66 (2017).

[18] Yaripour F., Shariatinia Z., Sahebdelfar S., Irandoukht A., Effect of Boron Incorporation on the Structure, Products Selectivities and Lifetime of H-ZSM-5 Nanocatalyst Designed for Application in Methanol-to-Olefins (MTO) Reaction, *Micropor. Mesopor. Mat.*, **203**: 41-53 (2015).

[19] Perry R.H., Green D.W., Maloney J.O., "Perry's Chemical Engineers' Handbook", Eighth Edition, McGraw-Hill, New York (2008).

[20] Yaws C.Y., "Chemical Properties Handbook: Physical, Thermodynamic, Environmental, Transport Safety and Health Related Properties for Organic and Inorganic Chemicals", McGraw- Hill Inc., New York (1998).

[21] Dahl I.M., Kolboe S., On the Reaction Mechanism for Hydrocarbon Formation from Methanol over SAPO-34: I. Isotopic Labeling Studies of the Co-Reaction of Ethane and Methanol, *J. Catal.*, **149**: 458-464 (1994).

[22] Farzi A., Jomea M.J., Simulation and Control of a Methanol-To-Olefins (MTO) Laboratory Fixed-Bed Reactor, *Iran. J. Chem. Chem. Eng. (IJCCE)*, **36**, 175-190 (2017).

[23] Lu J., Wang X., Li H., Catalytic Conversion of Methanol to Olefins over Rare Earth (La, Y) Modified SAPO-34, *React. Kin. Catal, Lett.*, **97**: 225-261 (2009).

[24] Wang P., Lv A., Hu J., Xu J., Lu G., The Synthesis of SAPO-34 with Mixed Template and Its Catalytic Performance for Methanol to Olefins Reaction. *Micropor. Mesopor. Mat.*, **152**: 178-184 (2012).

[25] Liu G., Tian P., Li J., Zhang D., Zhoub F., Liu Z., Synthesis, Characterization and Catalytic Properties of SAPO-34 Synthesized Using Diethylamine as a Template, *Micropor. Mesopor. Mat.*, **111**: 143-149 (2008).

[26] Wang P., Yang D., Hu J., Xu J., Lu G., Synthesis of SAPO-34 with Small and Tunable Crystallite Size by Two-step Hydrothermal Crystallization and Its Catalytic Performance for MTO Reaction, *Catal. Today.*, **212**: 62.e1-62.e8 (2013).

[27] Chang C.D., Silvestri A.J., The Conversion of Methanol and Other O-compounds to Hydrocarbons over Zeolite Catalysts, *J. Catal.*, **47**: 249-259 (1977).

[28] Gubisch D., Bandermann F., Conversion of Methanol to Light Olefins over Zeolite H-T, *Chem. Eng. Technol.* **12**: 155-161 (1989).

[29] Fougerit J.M., Gnep, N.S., Guisnet M., Selective Transformation of Methanol into Light Olefins over a Mordenite Catalyst: Reaction Scheme and Mechanism, *Micropor. Mesopor. Mat.*, **29**: 79-89 (1999).

[30] Zhao W., Zhang B., Wang G., Guo H., Methane Formation Route in the Conversion of Methanol to Hydrocarbons, *J. Energy Chem.*, **23**: 201-206 (2014).

[31] Wu E.L., Kuhl G.H., Whyte T.E., Venuto P.B., Molecular Sieve Zeolites-I, *Adv. Chem. Ser.*, **101**: 490-498 (1971).

[32] Haag W.O., Dessau R.M., "Proceedings of the Eighth International Congress on Catalysis", July 2-6, 1984, Berlin, Germany, Vol. 2, Verlag Chemie, Weinheim, p. 305 (1984).

[33] Chen D., Moljord K., Fuglerud T., Holmen A., The Effect of Crystal Size of SAPO-34 on the Selectivity and Deactivation of the MTO Reaction, *Micropor. Mesopor. Mat.*, **29**: 191-203 (1999).

[34] Hirota Y., Murata K., Miyamoto M., Egashira Y., Nishiyama N., Light Olefins Synthesis from Methanol and Dimethylether over SAPO-34 Nanocrystals, *Catal. Lett.*, **140**: 22-26 (2010).

[35] Wu X., Abraha M.G., Anthony R.G., Methanol conversion on SAPO-34: Reaction Condition for Fixed-bed Reactor, *Appl. Catal. A: Gen.*, **260**: 63-69 (2004).

[36] Askari S., Halladj R., Sohrabi M., Methanol Conversion to Light Olefins over Sonochemically Prepared SAPO-34 Nanocatalyst, *Micropor. Mesopor. Mat.*, **163**: 334-342 (2012).

[37] Chen D., Moljord K., Holmen A., A Methanol to Olefins Review: Diffusion, Coke Formation and Deactivation on SAPO Type Catalysts, *Micropor. Mesopor. Mat.*, **164**: 239–250 (2012).